Time-reversal RAP-MUSIC imaging

Alexandre Baussard, T. Boutin

Time-reversal RAP-MUSIC imaging

A. BAUSSARD* and T. BOUTIN

E^3I^2 laboratory – ENSIETA, 2 rue François Verny, 29806 Brest, France

(Received 7 March 2007; in final form 31 May 2007)

Time-reversal imaging with the MUltiple SIgnal Classification (MUSIC) method for the location of point targets was first proposed by Devaney *et al.* In this paper, a recursive time-reversal MUSIC algorithm is proposed. The considered approach is based on the Recursively Applied and Projected (RAP) MUSIC which was first introduced for magnetoencephalographic (MEG) data processing. The main goal of this contribution is to test and study a time-reversal RAP-MUSIC approach for target location and imaging.

1. Introduction

Time-Reversal (TR) MUltiple SIgnal Classification (MUSIC)-based location, imaging, and inverse scattering were first introduced in [1–3] for point scatterers (whose size is smaller than the wavelength). Recent work, in this area, deals with extended targets [4]. These methods are named 'time-reversal MUSIC' because both time-reversal methods and MUSIC can be explained using the eigenvalues of the time reversal operator. For point targets, the TR MUSIC techniques have shown their capabilities to detect and locate them. However, in some cases this approach is not able to detect too close targets.

In this contribution, a recursive MUSIC approach for time-reversal imaging is considered. Sequential MUSIC algorithms [5–7] were introduced in order to outperform the classical MUSIC approach when the source signals are highly correlated. In general, when uncorrelated sources are under study, MUSIC and recursive MUSIC methods lead to equivalent results. The paper will focus on the recursively applied and projected (RAP) MUSIC proposed for magnetoencephalographic (MEG) data processing in [5]. The general idea is based on a recursive procedure in which each source is found as the global maximizer of a recursively adjusted cost function. The changes are made after each source detection by projecting the signal space away from the subspace spanned by the founded sources.

In this paper, a time-reversal RAP-MUSIC imaging approach is considered in order to improve the MUSIC approach when targets are highly correlated. The paper is organized as follows. In section 2, the considered setup is described. Then, in section 3, the electromagnetic model and the multistatic matrix are presented. Section 4 gives an overview of TR imaging with MUSIC and presents the TR imaging method based on RAP-MUSIC. Some simulations and comments are proposed in section 5. Finally, section 6 gives some concluding remarks.

*Corresponding author. E-mail: baussaal@ensieta.fr

2. Problem statement

The considered experimental setup (see figure 1) consists of an array of N_s transmitting antennas and an array (which defines the Γ domain) of N_r receiving antennas (of the same type).

The target under consideration can be made of one or more dielectric and/or metallic objects. In the plane of illumination, a two-dimensional search domain (Ω) containing the target is considered. The embedding medium (Ω_b) is assumed to be of infinite extent and homogeneous, with given permittivity $\varepsilon_b = \varepsilon_0 \varepsilon_{r,b}$, and permeability $\mu = \mu_0$ (ε_0 and μ_0 being the permittivity and the permeability of the vacuum, respectively). The objects are assumed to be inhomogeneous nonmagnetic cylinders with complex-valued permittivity distribution $\varepsilon(\mathbf{r}) = \varepsilon_0 \varepsilon_r(\mathbf{r})$.

The emitters are individually excited and generate a transverse magnetic (TM) polarized electromagnetic wavefield e_l^{inc} that illuminates the medium. For each irradiation, the receiving antennas provide the total field e_l which is defined as

$$e_l = e_l^d + e_l^{\text{inc}}, \tag{1}$$

where e_l^d is the scattered field by the targets inside the medium.

For each excitation, taking into account an $\exp(-i\omega t)$ time-dependence, the direct scattering problem can be modeled via two coupled contrast-source integral relationships: the observation equation (2) and the coupling equation (3)

$$e_l^d(\mathbf{r} \in \Gamma) = k_0^2 \int_\Omega \chi(\mathbf{r}')\, e_l(\mathbf{r}')\, G(\mathbf{r}, \mathbf{r}')\, \mathrm{d}\mathbf{r}', \tag{2}$$

$$e_l(\mathbf{r} \in \Omega) = e_l^{\text{inc}} + k_0^2 \int_\Omega \chi(\mathbf{r}')\, e_l(\mathbf{r}')\, G(\mathbf{r}, \mathbf{r}')\, \mathrm{d}\mathbf{r}', \tag{3}$$

where $\chi(\mathbf{r}) = \varepsilon_r(\mathbf{r}) - \varepsilon_{r,b}$ denotes the permittivity contrast, $G(\mathbf{r}, \mathbf{r}')$ is the two-dimensional free-space Green's function and k_0 is the wavenumber in vacuum.

3. Time-reversal matrix

In this part, some common issues for the electromagnetic model and the time-reversal matrix are presented. It is an overview of well-known hypotheses and developments (see for example [1, 2, 8]).

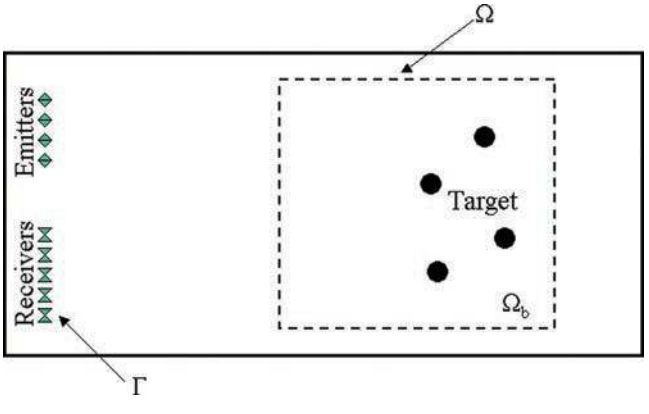

Figure 1. Experimental setup.

3.1 *Electromagnetic model*

In many works, the (first-order) Born approximation, which leads to neglect of the multiple scattering between targets, is considered. In this case, the effect of the target on the incident field is considered small so that the total field e_l in the observation equation (2) can be replaced by the incident field e_l^{inc}. In this contribution, the second-order scattering contribution is also take into account. Note that, in what follows, only one array of $N_s = N_r = N$ transceivers is considered; i.e. each antenna is an emitter and a receiver. The extension to one transmitting array and one receiving array can be easily done (see for example [2, 9]). Moreover, the sensors are considered small relative to the wavelength. In this case, the incident field is defined as

$$e_l^{\text{inc}}(r) = P_l G(r, R_l), \tag{4}$$

where P_l is the source excitation and R_l is the location of the transceiver l (used as emitter). From these hypotheses and considering M ($M < N$) point targets located at X_m, the scattered field can be expressed as

$$\begin{aligned} e_l^d(r) = &\sum_{m=1}^{M} G(r, X_m)\tau_m G(X_m, R_l)P_l \\ &+ \sum_{m=1}^{M}\sum_{m'=1}^{M} G(r, X_m)\tau_m G(X_m, R_l)\tau_{m'} G(X'_m, R_l)(1 - \delta_{m,m'})P_l, \end{aligned} \tag{5}$$

where τ_m is the scattering amplitude of the mth target and $\delta_{\dots}$ stands for the Kronecker symbol.

Note that a more complete model formulation through, for example, the Foldy–Lax multiple scattering model [10] can also be considered [9, 11]. But, from previous work on TR MUSIC, the performance of these approaches for target location seems to remain unchanged under a Born approximation or a non-Born approximation (multiple scattering) [11]. So we could also expect not a lot of modifications in our final results using our treatment with the 'Foldy–Lax model'.

3.2 *Time-reversal matrix*

The $[N \times N]$ multistatic response matrix $\mathbf{K}$, whose entry $K_{i,j}$ is defined as the value of the scattered field detected at the ith transceiver (used as receiver) due to the unit excitation at the jth transceiver (used as emitter), is given by

$$\mathbf{K} = \sum_{m=1}^{M} \tau_m \mathbf{g}_m \mathbf{g}_m^T + \sum_{m=1}^{M}\sum_{m'=1}^{M} \mathbf{g}_m \tau_m G(X_m, X_{m'})\tau_{m'}(1 - \delta_{m,m'})\mathbf{g}_{m'}^T. \tag{6}$$

where $\mathbf{g}_m^T$ denotes the transpose of $\mathbf{g}_m$ which is the N-dimensional Green function column vector:

$$\mathbf{g}_m = \begin{bmatrix} G(R_1, X_m) \\ G(R_2, X_m) \\ \vdots \\ G(R_N, X_m) \end{bmatrix}. \tag{7}$$

Finally, the time-reversal matrix is defined as

$$\mathbf{T} = \mathbf{K}^{\dagger}\mathbf{K}, \tag{8}$$

where $\dagger$ stands for the adjoint operator.

4. Time-reversal RAP-MUSIC imaging

4.1 *Time-reversal MUSIC imaging (overview)*

Time-reversal imaging using MUSIC was first proposed in [3]. This signal subspace method assumes that the number of point targets N_c in the medium is lower than the number of transceivers. The general idea is to localize multiple sources by exploiting the eigenstructure of the time-reversal matrix.

Performing the SVD on the time-reversal matrix, the space C of voltage vectors applied to the N-transceiver array can be decomposed into the direct sum $C = S \oplus B$, where the signal subspace S is orthogonal to the noise subspace B, where S is spanned by the principal eigenvectors μ_i of the TR matrix having nonzero eigenvalues. B is spanned by the eigenvectors μ_i of T having zero eigenvalues.

Let $\hat{N}_c$ be the number of nonzero eigenvalues, i.e. the estimated number of targets inside the medium.

It follows from the orthogonality of the signal and noise subspaces that the target locations must correspond to the poles (peaks) in the MUSIC pseudo-spectrum:

$$P^{\mathrm{MUSIC}}(\mathbf{r}) = \frac{1}{\sum_{m=\hat{N}_c+1}^{N} |\langle \mu_m^{\dagger}, \mathbf{g}_d^*(\mathbf{r})\rangle|^2}, \tag{9}$$

where for all $m = \hat{N}_c + 1, \ldots, N$ the inner product $\langle \mu_m^{\dagger}, \mathbf{g}_d^*(\mathbf{r})\rangle = 0$ whenever $\mathbf{r}$ is the actual location of one of the targets. $\mathbf{g}_d(\mathbf{r})$ corresponds to the Green function in the free space.

4.2 *Time-reversal RAP-MUSIC imaging*

The recursively applied and projected (RAP) MUSIC method uses each successively located source to form an intermediate array gain matrix and projects the array manifold and the estimated signal subspace into its orthogonal complement. MUSIC is then performed in this reduced subspace to find the next source.

The kth ($k = 1, \ldots, \hat{N}_c$) iteration of the proposed time-reversal RAP-MUSIC algorithm is:

$$\hat{\mathbf{r}}_k = \max_{\mathbf{r}}(c_k(\mathbf{r})), \tag{10}$$

where c is the subspace correlation coefficient (see [5, 6]) defined as

$$c_k(\mathbf{r}) = \mathrm{subcorr}\Big(\Pi^{\perp}_{\hat{\mathbf{G}}_{k-1}} \mathbf{g}_d^*(\mathbf{r}),\, \Pi^{\perp}_{\hat{\mathbf{G}}_{k-1}} \mathcal{S}\Big). \tag{11}$$

$\Pi^{\perp}$ denotes the orthogonal projector given by

$$\Pi^{\perp}_{\hat{\mathbf{G}}_{k-1}} = \mathbf{I} - \hat{\mathbf{G}}_{k-1}\big(\hat{\mathbf{G}}_{k-1}^H \hat{\mathbf{G}}_{k-1}\big)^{-1} \hat{\mathbf{G}}_{k-1}^H, \tag{12}$$

and

$$\hat{\mathbf{G}}_{k-1} = [\mathbf{g}_d^*(\mathbf{r}_1)\ \ldots\ \mathbf{g}_d^*(\mathbf{r}_{k-1})]. \tag{13}$$

Finally, the image of the observed medium (see section 5.) at iteration k is obtained by using the pseudo-spectrum P^{RM} defined as

$$P_k^{\mathrm{RM}}(\mathbf{r}) = \frac{1}{\sqrt{1 - c_k^2(\mathbf{r})}}. \tag{14}$$

P^{RM} tends towards infinity when $c = 1$ (the two considered subspaces have at least a common subspace) and towards 1 when $c = 0$ (the two subspaces are orthogonal).

The process can be stopped when at the iteration i where no c-values greater than a given threshold c_{th} exist, i.e. it is not possible to detect another target:

$$\max_{\mathbf{r}}(c_k(\mathbf{r})) < c_{\mathrm{th}}, \tag{15}$$

where c_{th}, in our simulations, was fixed to 0.95. This value seems to be efficient in all our simulations (even those which are not presented in this paper).

5. Simulations

Note that all the presented images are normalized and that white-noise (around 20 dB) has been added to the analytically obtained forward data signals before treatment. The used point targets have the same scattering amplitude.

5.1 *Time-reversal RAP-MUSIC algorithm*

In this part, the TR RAP-MUSIC algorithm is presented through simulation results. The considered configuration is made of $N = 9$ transceivers equally spaced and separated by $\lambda/2$. Only two targets separated by λ are under consideration (see figure 2). The work frequency is fixed to 200 MHz. This first configuration is not a challenging one but it is used in order to clearly present how the proposed algorithm works.

At the end of the first iteration of the algorithm and from the pseudo-spectrum P^{RM} (see figure 3a), the two targets can be easily seen. In figure 3(b), the subspace correlation coefficients are shown. From this first step $\hat{r}_1$ (i.e the position of a target) is extracted and the orthogonal projector is constructed.

At the end of the second step (figure 4a), only one target can be seen. This means that the target (source) has been clearly detected and the signal space has been perfectly projected away from the subspace spanned by the (previous) founded source. Figure 4(b) shows the subspace correlation coefficients.

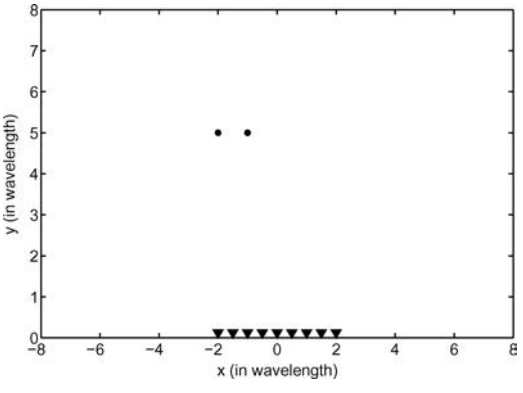

Figure 2. Configuration I: the • and the black ∇ stand respectively for a target location and an antenna location.

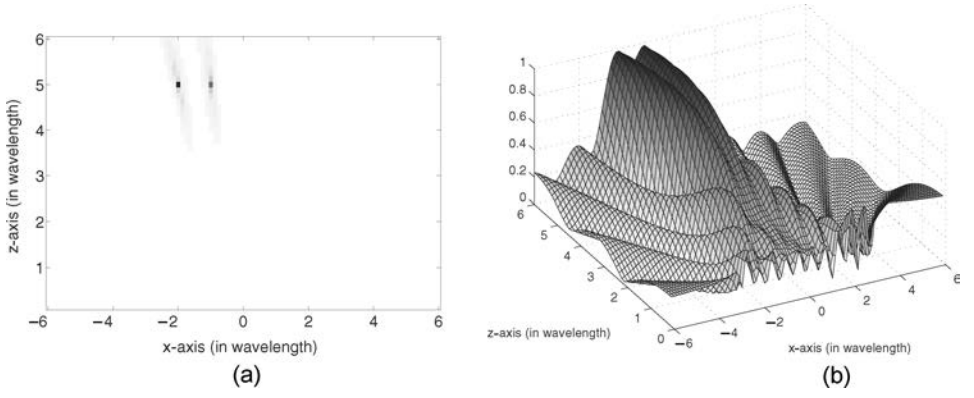

Figure 3. Time-reversal RAP-MUSIC results for configuration I at iteration 1. (a) Pseudo-spectrum; (b) subspace correlation coefficients.

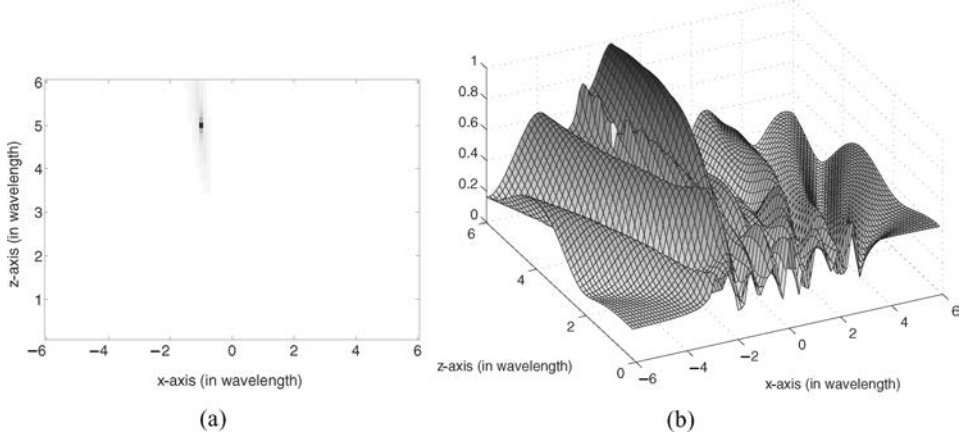

Figure 4. Time-reversal RAP-MUSIC results for configuration I at iteration 2. (a) Pseudo-spectrum; (b) subspace correlation coefficients.

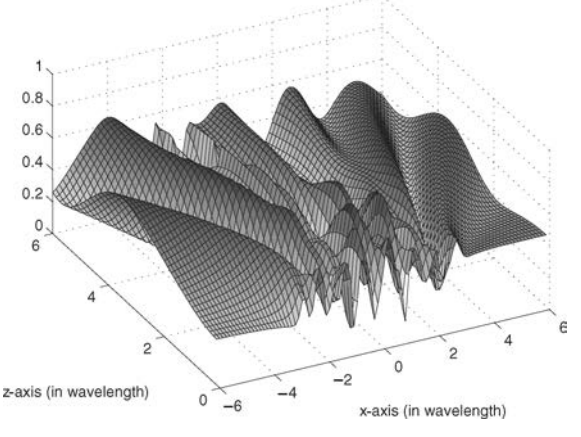

Figure 5. Subspace correlation coefficients at iteration 3 for configuration I.

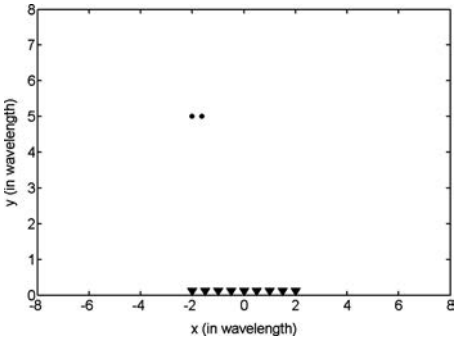

Figure 6. Configuration II: the • and the black ∇ stand respectively for a target location and an antenna location.

If another iteration is performed, the second target is perfectly detected (by the algorithm) and no more c-values are greater than c_{th} (see figure 5), which means that (for the detection algorithm) no more targets are in the medium.

5.2 *Comparison between TR MUSIC and TR RAP-MUSIC*

The proposed configuration in this part is more challenging than in the previous one. Here, the two targets are separated by $\lambda/3$ (see figure 6). The search domain has been discretized into square pixels (size $= \lambda/10$). For both algorithms the number of targets inside the medium is assumed to be known.

In this case, from figure 7, using the MUSIC approach we are not able to clearly see the two targets.

Figures 8 and 9(a) show the results obtained respectively at iteration 1 and at iteration 2 of the RAP-MUSIC approach. Figure 9(b) corresponds to the subtraction of the result at iteration 1 from the result at iteration 2. This figure allows us to clearly see that RAP-MUSIC has correctly localized and detected the first target at the end of iteration 1.

These results show that RAP-MUSIC, contrary to MUSIC, is able to clearly detect and localize both targets (see figure 9a, b and table 1).

Note that if a third iteration of the proposed algorithm is performed no more targets can be detected (all the c-values are lower than c_{th}).

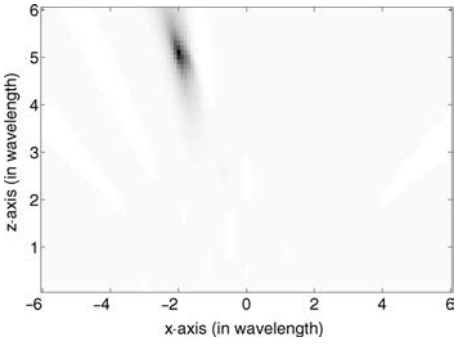

Figure 7. Configuration II: time-reversal MUSIC result.

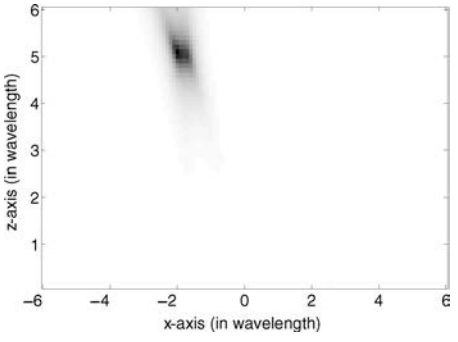

Figure 8. Configuration II: time-reversal RAP-MUSIC result at iteration 1.

5.3 *Time-reversal RAP-MUSIC imaging analysis*

In this part some complementary remarks are proposed in order to detail the analysis of the proposed approach.

In fact for highly noisy data, as shown before, RAP-MUSIC is able to detect really close targets. However, in some cases the location of these targets can be damaged. Since one of the steps of RAP-MUSIC is based on a maximization, it may occur that the maximum cannot be found at one of the target positions, but rather at a location between the two targets. In this case, a wrong projector is constructed.

Let us do the same simulation as the previous one but with 15 dB noisy data. In this case, as shown in figures 10 and 11 and in table 2, the two targets are detected but the position of the first one is not well estimated. It follows that the projector operator is not well constructed which leads to damage in the detection of the second target (see figure 10). Moreover, in this case, at the end of the second iteration, the pseudo-spectrum shows two different spots. Fortunately in the proposed simulation, only the two targets are detected. Actually, the subspace correlation coefficients at the third iteration are lower than c_{th} which means that no more targets can be found (i.e. the algorithm does not find that the two spots at the previous iteration are two real targets). Unfortunately, in some cases the wrong estimation of the target positions and so the construction of the projector operators could finally lead to estimating three or more targets or to cause the algorithm to strongly fail.

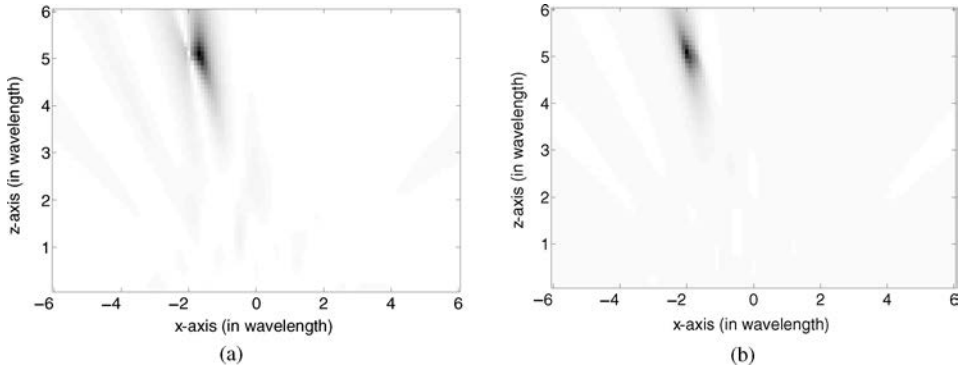

Figure 9. Time-reversal RAP-MUSIC results for configuration II: (a) iteration 2; (b) first detected target (subtraction between figure 8 and figure 9a).

Table 1. True position of the targets in the medium and estimated position after detection.

	Target 1	Target 2
True location	$(x = -1.66\lambda, z = 5\lambda)$	$(x = -2\lambda, z = 5\lambda)$
Estimated location	$(x = -1.7\lambda, z = 5.1\lambda)$	$(x = -2\lambda, z = 5.1\lambda)$

Table 2. True position of the targets in the medium and estimated position after detection.

	Target 1	Target 2
True location	$(x = -1.66\lambda, z = 5\lambda)$	$(x = -2\lambda, z = 5\lambda)$
Estimated location	$(x = -1.8\lambda, z = 4.9\lambda)$	$(x = -1.9\lambda, z = 4.8\lambda)$

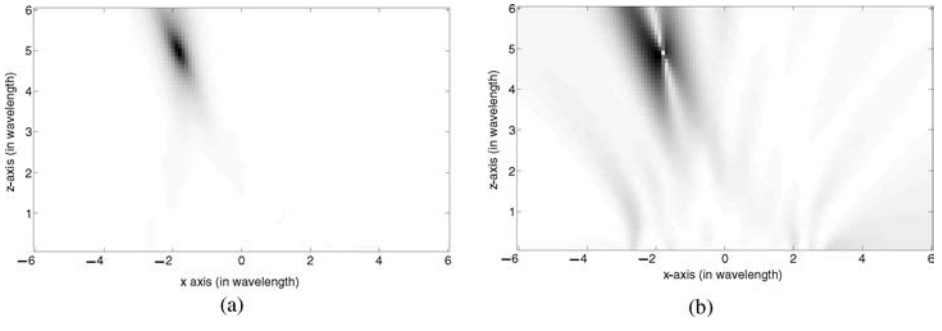

Figure 10. Time-reversal RAP-MUSIC results for configuration II with 15dB noisy data: (a) iteration 1; (b) iteration 2.

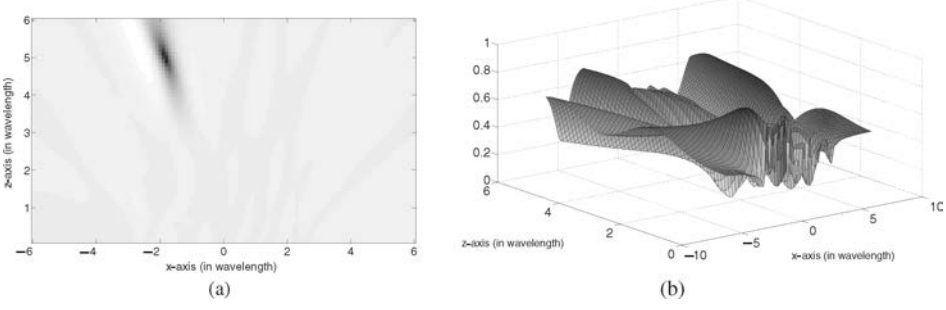

Figure 11. Time-reversal RAP-MUSIC results for configuration II with 15dB noised data: (a) first detected target (subtraction between result from figure 10a and result from figure 10b); (b) subspace correlation coefficients at iteration 3.

As this can be a problem in some applications, complementary work should be developed in order to solve it and so obtain a perfect localization of the targets in these particular challenging cases.

Finally, one can also note that in equation (6), the term with the double sum may have an effect similar to the presence of a non-white noise component. In this case, we are not in the optimal conditions for a MUSIC type approach. In this way, it could be interesting to focus on some work using [12–14].

6. Conclusions and further work

In this contribution, a time-reversal recursively applied and projected (RAP) MUSIC was considered. The proposed results show that RAP-MUSIC outperforms the classical MUSIC approach when targets are strongly correlated. However, we noted that errors could appear when dealing with highly noisy data. The challenging point in the proposed approach is the estimation of the subspace correlation coefficient maximum which acts upon the projector operators and the targets locations.

Like for the MUSIC algorithm, this approach is limited to $M < N$ and the obtained results depend on the noise signal subspace estimation (which remain a challenging problem). However, because of the recursive approach, RAP-MUSIC could be less sensitive about this estimate (when the signal subspace rank is overestimated) than MUSIC. Some further work could focus on this point and try to take advantage of the recursive approach.

References

[1] Gruber, F. K., Marengo, E. A. and Devaney, A. J., 2004, Time-reversal imaging with multiple signal classification considering multiple scattering between the targets. *Journal of the Acoustical Society of America*, **115**, 3042–3047.

[2] Lehman, S. K. and Devaney, A. J., 2003, Transmission mode time-reversal super-resolution imaging. *Journal of the Acoustical Society of America*, **113**, 2742–2753.

[3] Lev-Ari, H. and Devaney, A. J., 2000, The time-reversal technique reinterpreted: Subspace-based signal processing for multi-static target location. *IEEE Sensor Array and Multichannel Signal Processing Workshop*, Cambridge (MA), USA, 509–513.

[4] Marengo, E. A., Gruber, F. K. and Simonetti, F., Time-reversal MUSIC imaging of extended targets. To be published in *IEEE trans. Image Processing*.

[5] Mosher, J. C. and Leahy, R. M., 1998, Recursive MUSIC: A framework for EEG and MEG source localization. *IEEE trans. Biomedical Engineering*, **45**(11), 1342–1354.

[6] Mosher, J. C. and Leahy, R. M., 1999, Source localization using Recursively Applied and Projected (RAP) MUSIC. *IEEE trans. Signal Processing*, **47**(2), 332–340.

[7] Stoica, P., Handel, P. and Nehorai, A., 1995, Improved sequential MUSIC. *IEEE Trans. Aerospace and Electronic Systems*, **31**(4), 1230–1239.

[8] Borcea, L., Papanicolaou, G., Tsogka, C. and Berryman, J., 2002, Imaging and time-reversal in random media. *Inverse Problems*, **18**, 1247–1279.

[9] Marengo, E. A. and Gruber, F. K., 2007, Subspace-based localization and inverse scattering of multiply scattering point targets. *EURASIP Journal on Advances in Signal Processing*, **Article ID 17342**.

[10] Taylor, J. H., 1972, *Scattering theory* (New York: Wiley).

[11] Marengo, E. A., 2005, Single-snapshot signal subspace methods for active target location: Part I: Multiple scattering case. Proceedings of the Second IASTED International Conference on Antennas, Radar and Wave Propagation, 161–166, Banff, Canada, 19–21 July.

[12] Byrne, C. L. and Steele, A. K. 1985, Stable nonlinear methods for sensor array processing. *IEEE Journal of Oceanic Engineering*, **OE-10**(3), 255–259.

[13] Steele, A. K. and C. L. Byrne, 1990, High-resolution array processing using implicit eigenvector weighting techniques. *IEEE Journal of Oceanic Engineering*, **15**(1), 8–13.

[14] Steele, A. K. and C. L. Byrne, 1993, Performance comparison of high resolution bearing estimation algorithms using simulated and sea test data. *IEEE Journal of Oceanic Engineering*, **18**(4), 438–446.